



## Detection of Diabetic Wounds Based on Segmentation Using Accelerated Mean Shift Algorithm

<sup>1</sup>M. Saratha, <sup>2</sup>V. Mohana Priya

<sup>1</sup>B. Tech, M.E., Department of Computer Science and Engineering, Anna University  
Staff member of Vivekanandha College of Technology for Women, Sathinaickanpalayam,  
Tiruchengode, Tamilnadu, India

<sup>2</sup>M.E., Department Of Computer Science and Engineering, Anna University  
PG Scholar of Vivekanandha College of Technology for Women, Sathinaickanpalayam,  
Tiruchengode, Tamilnadu, India

---

**Abstract**—*Diabetic foot ulcers represent a significant health issue. Currently, clinicians and nurses mainly base their wound assessment on visual examination of wound size and healing status, while the patients themselves seldom have an opportunity to play an active role. Hence, a more quantitative and cost-effective examination method that enables the patients and their caregivers to take a more active role in daily wound care potentially can accelerate wound healing, save travel cost and reduce healthcare expenses. This proposed novel has a wound image which is captured by the camera. After that, the system performs wound segmentation by applying the accelerated mean shift algorithm. Specifically, the outline of the foot is determined based on the wound boundary is found using a simple connected region detection method. Within the wound boundary, the healing status is next assessed based on red–yellow–black color evaluation model. Moreover, the healing status is quantitatively assessed, based on trend analysis of time records for a given patient. Experimental results on wound images collected in UMASS—Memorial Health Center Wound Clinic (Worcester, MA) following an Institutional Review Board approved protocol show that our system can be efficiently used to analyze the wound healing status with promising accuracy.*

**Keywords**— *Mean shift algorithm, Wound segmentation, Healing status, Maximum Likelihood principle, Risk analysis.*

---

### I. INTRODUCTION

For individuals with type 2 diabetes, foot ulcers constitute a significant health issue affecting 5–6 million individuals in the US [1], [2]. Foot ulcers are painful, susceptible to infection and very slow to heal [3], [4]. According to published statistics, diabetes-related wounds are the primary cause of nontraumatic lower limb amputations with approximately 71 000 such amputations in the US in 2004 [5]. Moreover, the cost of treating diabetic foot ulcers is estimated at \$15 000 per year per individual. Overall diabetes healthcare cost was estimated at \$245 billion in 2012 and is expected to increase in the coming years [5].

There are several problems with current practices for treating diabetic foot ulcers. First, patients must go to their wound clinic on a regular basis to have their wounds checked by their clinicians. This need for frequent clinical evaluation is not only inconvenient and time consuming for patients and clinicians, but also represents a significant health care cost because patients may require special transportation, e.g., ambulances. Second, a clinician's wound assessment process is based on visual examination.

Bob Zhang [1] has described about Diabetes mellitus (DM) and its complications leading to diabetic retinopathy (DR) are soon to become one of the 21st century's major health problems. This represents a huge financial burden to healthcare officials and governments. To combat this approaching epidemic, this paper proposes a noninvasive method to detect DM and nonproliferative diabetic retinopathy (NPDR), the initial stage of DR based on three groups of features extracted from tongue images. They include color, texture, and geometry

Lucas [2] has said that in telemedicine environments, a standardized and reproducible assessment of wounds, using a simple free-handled digital camera, is an essential requirement. However, to ensure robust tissue classification, we introduce the key steps including color correction, and segmentation-driven classification based on support vector machines. The tool thus developed ensures stability under lighting condition, viewpoint, and camera changes, to achieve accurate and robust classification of skin tissues. Clinical tests demonstrate that such an advanced tool, which forms part of a complete 3-D and color wound assessment system, significantly improves the monitoring of the healing process. It achieves an overlap score of 79.3 against 69.1% for a single expert.

Gui and Xu .C. F. [3] has used Level set methods in image processing and computer vision. In conventional level set formulations, the level set function typically develops irregularities during its evolution, which may cause numerical errors and eventually destroy the stability of the evolution. This paper proposes a new variational level set formulation in which the regularity of the level set function is intrinsically maintained during the level set evolution.

Comaniciu and P. Meer [4] said that Numerous nonparametric clustering methods can be separated into two parts: hierarchical clustering and density estimation. Hierarchical clustering composes either 23 aggregation or division based on some proximate measure. The concept of the density estimation-based nonparametric clustering method is that the feature space can be considered as the experiential probability density function (p.d.f.) of the represented parameter. The mean shift algorithm can be classified as density estimation. It adequately analyzes feature space to cluster them and can provide reliable solutions for many vision tasks.

Wang .L, Pedersen .P .C, Strong .D, Tulu .B, and Agu .E [5] Considering the prevalence of smartphones with a high- resolution digital camera, assessing wounds by analyzing images of chronic foot ulcers is an attractive option. In this paper, we propose a novel wound image analysis system implemented solely on the Android smartphone. The wound image is captured by the camera on the smartphone with the assistance of an image capture box.

## II. WOUND ANALYSIS METHOD

### A. Wound Image Analysis System Overview

Our quantitative wound assessment system consists of several functional modules including wound image capture, wound image storage, wound image preprocessing, wound boundary determination, wound analysis by color segmentation and wound trend analysis based on a time sequence of wound images for a given patient. The functional diagram of our quantitative wound assessment system is shown as in Fig. 1

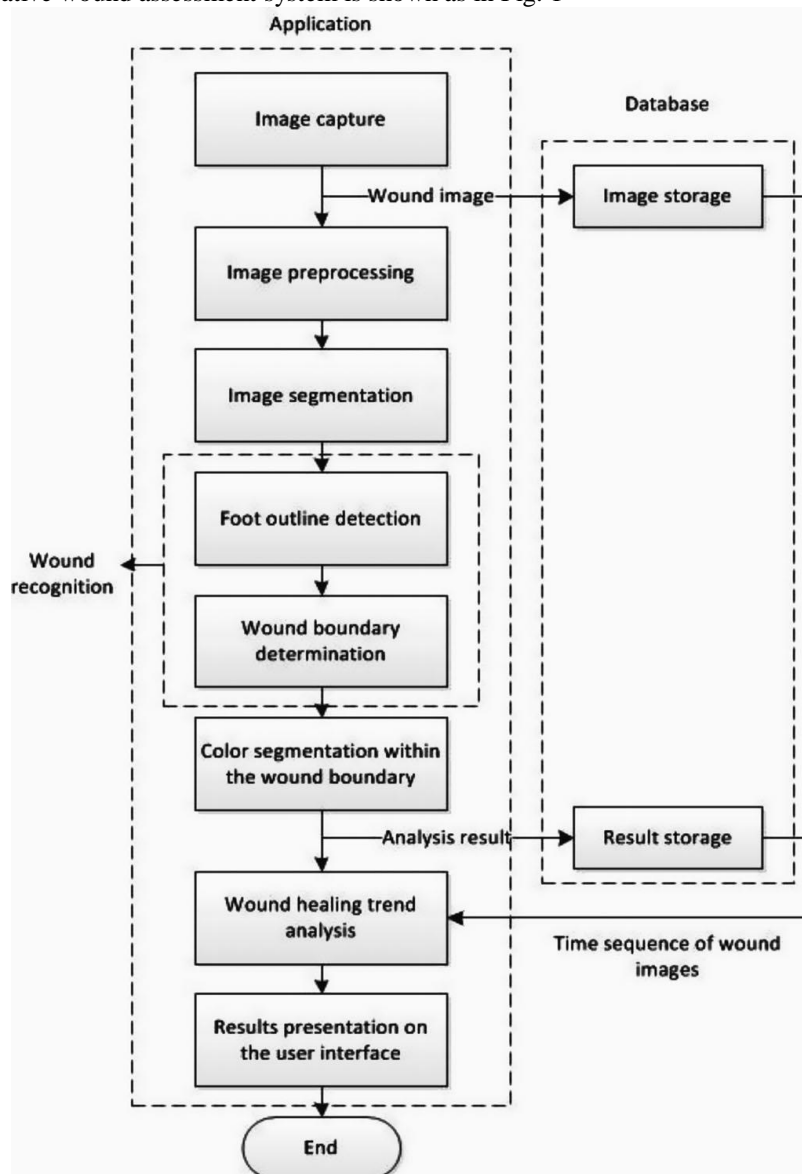


Fig.1. Woundimage analysis system software.

After the wound image is captured, the JPEG file path of this image is added into a wound image database. To determine the boundary of the wound area, we first determine an outline of the foot within the image. Hence the initial *Image*

segmentation operation is to divide the original image into pixel groups with homogeneous color values. Based on the standard color checkers provided in [20], both the light and dark skin color thresholds in CIE LAB space are incorporated into the system, which means that our algorithm is expected to work for most skin colors.

Afterwards, we carry out a *Wound boundary determination* based on the foot outline detection result. If the foot detection result is regarded as a binary image with the foot area marked as “white” and rest part marked as “black,” it is easy to locate the wound boundary within the foot region boundary by detecting the largest connected “black” component within the “white” part. If the wound is located at the foot region boundary, then the foot boundary is not closed, and hence the problem becomes more complicated, i.e., we might need to first form a closed boundary. When the wound boundary has been successfully determined and the wound area calculated, we next evaluate the healing state of the wound by performing *Color segmentation*, with the goal of categorizing each pixel in the wound boundary into certain classes labeled as granulation, slough and necrosis [21], [24]. After the color segmentation, a feature vector including the wound area size and dimensions for different types of wound tissues is formed to describe the wound quantitatively. This feature vector, along with both the original and analyzed images, is saved in the result database.

### B. Mean-Shift-Based Segmentation Algorithm

I chose the mean-shift algorithm, proposed in [16], over other segmentation methods. The mean-shift filtering algorithm is suitable for parallel implementation since the basic processing unit is the pixel. The mean-shift algorithm belongs to the density estimation based nonparametric clustering methods, in which the feature space can be considered as the empirical probability density function of the represented parameter. In general, the mean-shift algorithm models the feature vectors associated with each pixel (e.g., color and position in the image grid) as samples from an unknown probability density function  $f(x)$  and then finds clusters in this distribution. The center for each cluster is called the mode [25]. Given  $n$  data points  $x_i, i = 1, \dots, n$  in the  $d$ -dimensional space  $R^d$ , the multivariate kernel density estimator

$$f_h(x) = \frac{c_{k,d}}{nh^d} \sum_{i=1}^n k\left(\frac{x-x_i}{h}\right)^2 \quad (1)$$

where  $g(r) = -k'(r)$  and  $n$  is the number of neighbors taken into account in the five dimension sample domain. We use the combined kernel function where  $h_s$  and  $h_r$  are different bandwidth values for spatial domain and range domain, respectively. The vector  $k(x)$  defined in (1) is called the mean-shift vector, since it is the difference between the current value  $x$  and the weighted mean of the neighbors  $x_i$  around  $x$ . In the mean-shift procedure, the current estimate of the mode  $y^k$  at iteration  $k$  is replaced by its locally weighted mean

$$y^{k+1} = y^k + m(y^k) \quad (2)$$

This iterative update of the local maxima estimation will be continued until the convergence condition is met

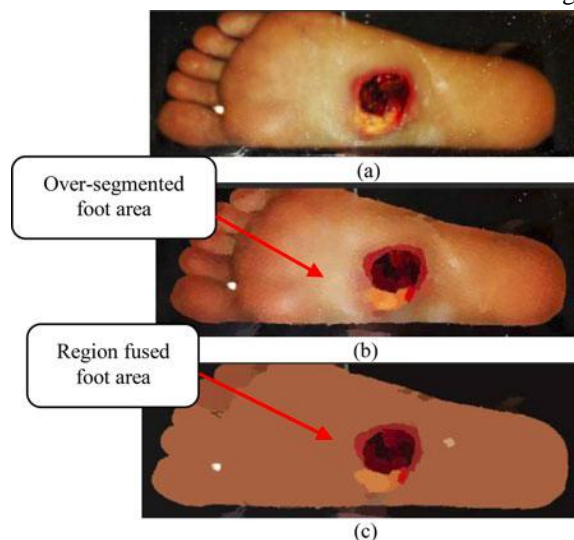


Fig.2. Mean-shift-based image segmentation sample result. (a) Original image.

- (b) Mean-shift-filtered image
- (c) Region fused image..

The color difference between two adjacent nodes should not exceed  $hf$ , which is regarded as the region fusion resolution. The mean-shift filtering and region fusion results of a sample foot wound are shown. We can see that the over-segmentation problem in (b) is effectively solved by region fusion procedure.

### C. Wound Boundary Determination and Analysis Algorithms

Based on the camera screen resolution, skin color feature and foot outline assumptions, the proposed wound boundary determination method is illustrated as in Fig. 3, and explained next. The *Largest connected component detection* is first performed on the segmented image, using the fast largest connected component detection method introduced in [31] including two passes.

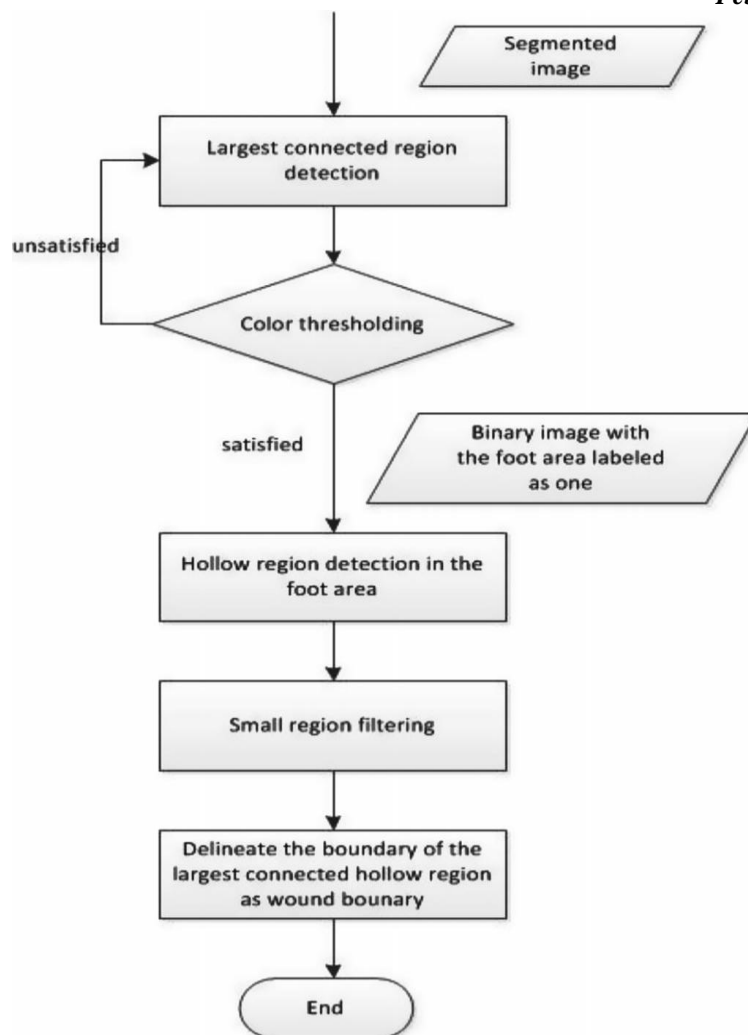


Fig.3. Largest connected component detection-based wound boundary determination method flowchart

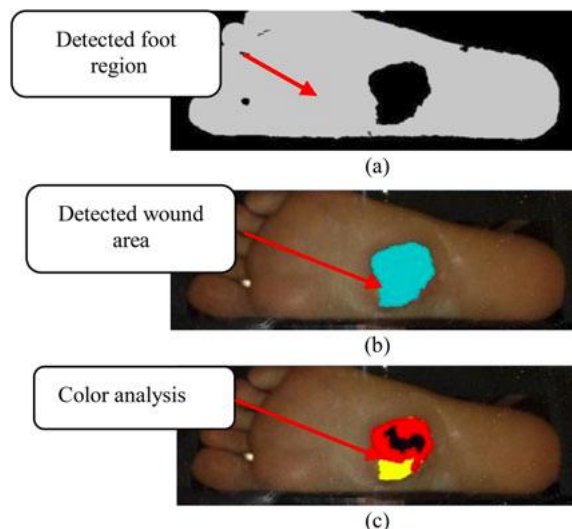


Fig.4. Wound boundary determination and analysis result. (a) Foot boundary detection result. (b) Wound boundary determination result. (c) Color segmentation result within the wound boundary

After the best estimate of the wound boundary is obtained, we analyze the wound area within the boundary using a wound description model.

### III. WOUND COLOR FEATURES

The following section describes how color features are extracted from tongue images. Every foreground tongue pixel is compared to 12 colors representing the tongue color gamut and assigned its nearest color. This forms the color features.

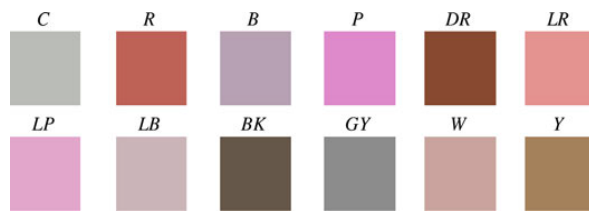


Table I RGB and CIELAB Values of the 12 Colors

Color	[R G B]	[L A B]
C (Cyan)	[188 188 185]	[76.0693 -0.5580 1.3615]
R (Red)	[189 99 91]	[52.2540 34.8412 21.3002]
B (Blue)	[183 165 180]	[69.4695 9.5423 -5.4951]
P (Purple)	[226 142 214]	[69.4695 42.4732 -23.8880]
DR (Deep red)	[136 72 49]	[37.8424 24.5503 25.9396]
LR (Light red)	[227 150 147]	[69.4695 28.4947 13.3940]
LP (Light purple)	[225 173 207]	[76.0693 24.3246 -9.7749]
LB (Light blue)	[204 183 186]	[76.0693 7.8917 0.9885]
BK (Black)	[107 86 56]	[37.8424 3.9632 20.5874]
GY (Gray)	[163 146 143]	[61.6542 5.7160 3.7317]
W (White)	[200 167 160]	[70.9763 10.9843 8.2952]
Y (Yellow)	[166 129 93]	[56.3164 9.5539 24.4546]

### A. Color Feature Extraction

For the foreground pixels of a tongue image, corresponding RGB values are first extracted, and converted to CIELAB [29] by transferring RGB to CIEXYZ using

$$\begin{bmatrix} X \\ Y \\ Z \end{bmatrix} = \begin{bmatrix} 0.4124 & 0.3576 & 0.1805 \\ 0.2126 & 0.7152 & 0.0722 \\ 0.0193 & 0.1192 & 0.9505 \end{bmatrix} \begin{bmatrix} R \\ G \\ B \end{bmatrix}$$

followed by CIEXYZ to CIELAB via

$$\begin{aligned} L^* &= 166 \cdot f(Y/Y_0) - 16 \\ a^* &= 500 \cdot [f(X/X_0) - f(Y/Y_0)] \\ b^* &= 200 \cdot [f(Y/Y_0) - f(Z/Z_0)] \end{aligned}$$

where  $f(x) = x^{1/3}$  if  $x > 0.008856$  or  $f(x) = 7.787x + 16/116$  if  $x \leq 0.008856$ .

$X_0$ ,  $Y_0$ , and  $Z_0$  in (2) are the CIEXYZ tristimulus values of the reference white point. The LAB values are then compared to 12 colors from the foot color gamut (see Table I) and assigned the color which is closest to it (measured using Euclidean distance). After evaluating all foot foreground pixels, the total of each color is summed and divided by the total number of pixels. This ratio of the 12 colors forms the foot color feature vector  $v$ , where  $v = [c_1, c_2, c_3, c_4, c_5, c_6, c_7, c_8, c_9, c_{10}, c_{11}, c_{12}]$  and  $c_i$  represents the sequence of colors in Table I. The original image is decomposed into one of the 12. Only seven colors are listed out of the 12 as the remaining five have ratios less than 1%

### B. Foot Texture Features

Texture feature extraction from wound images is presented in this section. To better represent the texture of wound images, eight blocks of size  $64 \times 64$  strategically located on the foot surface are used. A block size of  $64 \times 64$  was chosen due to the fact that it covers all eight surface areas very well, while achieving minimum overlap. Larger blocks would cover areas outside the wound boundary, and overlap more with other blocks. Smaller block sizes would prevent overlapping, but not cover the eight areas as efficiently. The blocks are calculated automatically by first locating the center of the wound using a segmented binary foot foreground image. Following this, the edges of the wound are established and equal parts are measured from its center to position the eight blocks. The Gabor filter is a linear filter used in image processing, and is commonly used in texture representation. To compute the texture value of each block, the 2D Gabor filter is applied and defined as  $G_k$

$$G_k(x, y) = \exp\left(-\frac{x^2}{2\sigma^2} - \frac{y^2}{2\sigma^2}\right) \cos\left(\frac{2\pi}{\lambda}(x \cos\theta + y \sin\theta)\right) \quad (3)$$

$$\begin{aligned} x_+ &= x \cdot \cos\theta + y \cdot \sin\theta \\ y_+ &= -x \cdot \sin\theta + y \cdot \cos\theta \end{aligned}$$

$\sigma$  is the variance,  $\lambda$  is the wavelength,  $\gamma$  is the aspect ratio of the sinusoidal function, and  $\theta$  is the orientation. A total of three  $\sigma$  (1, 2, and 3) and four  $\theta$  ( $0^\circ$ ,  $45^\circ$ ,  $90^\circ$ , and  $135^\circ$ ) choices were investigated to achieve the best result. Each filter is convolved with a texture block to produce a response  $R_k(x, y)$ :

$$R_k(x, y) = G_k(x, y) * im(x, y) \quad (4)$$

where  $im(x, y)$  is the texture block and  $*$  represents 2-D convolution. Responses of a block are combined to form  $FR_i$ , and its final response evaluated as follows:

$$FRi(x, y) = \max (R1 (x, y), R2 (x, y), \dots, Rn(x, y)) \quad (5)$$

which selects the maximum pixel intensities, and represents the texture of a block by averaging the pixel values of  $FRi$ . In the end,  $\sigma$  equal to 1 and 2 with three orientations ( $45^\circ$ ,  $90^\circ$ , and  $135^\circ$ ) was chosen. This is due to the fact that the sum of all texture blocks between Healthy and DM had the largest absolute difference.

### C. Wound Geometry Features

In the following section, we describe geometry features extracted from wound images. These features are based on measurements, distances, areas, and their ratios.

**Width:** The width  $w$  feature is measured as the horizontal distance along the  $x$ -axis from a wound's furthest right edge point ( $x_{max}$ ) to its furthest left edge point ( $x_{min}$ ):

$$w = x_{max} - x_{min}. \quad (6)$$

**Length:** The length  $l$  feature is measured as the vertical distance along the  $y$ -axis from a wound's furthest bottom edge ( $y_{max}$ ) point to its furthest top edge point ( $y_{min}$ ):

$$l = y_{max} - y_{min}. \quad (7)$$

**Length-width ratio:** The length-width ratio  $lw$  is the ratio of a wound length to its width

$$lw = l/w. \quad (8)$$

**Smaller half-distance:** Smaller half-distance  $z$  is the half distance of  $l$  or  $w$  depending on which segment is shorter

$$z = \min (l, w) / 2. \quad (9)$$

**Center distance:** The center distance ( $cd$ ) is distance from  $w_{sy}$ -axis center point to the center point of

$$l(y_{cp})cd = (\max (y_{x_{max}}) + \max (y_{x_{min}})) / 2 - y_{cp} \quad (10)$$

where  $y_{cp} = (y_{max} + y_{min}) / 2$ .

**Center distance ratio:** Center distance ratio ( $cdr$ ) is ratio of  $cd$  to  $l$ :

$$cdr = cd/l. \quad (11)$$

**Area:** The area ( $a$ ) of a wound is defined as the number of foot foreground pixels.

**Circle area:** Circle area ( $ca$ ) is the area of a circle within the wound foreground using smaller half-distance  $z$ , where  $r = z$   
 $ca = \pi r^2$ . (12)

## IV. EXPERIMENTAL RESULTS

The goal of the experimental work has been:

- 1) to assess the accuracy of the wound boundary determination based on the mean-shift algorithm and the color segmentation based on the mean shift algorithm; and
- 2) to perform an efficiency colour feature extraction and analysis the healing status of the wound in a foot area by comparing the values to the CIE LAB values.

## V. CONCLUSION

we plan to apply machine learning methods to train the wound analysis system based on clinical input and hopefully thereby achieve better boundary determination results with less restrictive assumptions. Furthermore, we plan to compute a healing score to be assigned to each wound image to support trend analysis of a wound's healing status.

## REFERENCES

- [1] Agu E, Wang L, Pedersen P C, Strong D, and Tulu B (2013) 'Smart phone based wound assessment system for diabetic patients,'
- [2] Bob Zhang, Vijaya Kumar B V, and David Zhang (2014) 'Detecting Diabetes Mellitus and Non proliferative Diabetic Retinopathy Using Tongue Color Texture and Geometry Features'
- [3] Cheng Y Z (2015) 'Mean shift, mode seeking, and clustering,' IEEE Trans. Pattern Anal. Mach. Intell., vol. 17, no. 8, pp. 790-799.
- [4] Christoudias C M, Georgescu B and Meer P (2012) 'Synergism in low level vision,' in Proc. IEEE 16th Int. Conf. Pattern Recog., vol. 4, 2012, pp. 150-155.
- [5] Comaniciu D and Meer P (2012) Mean shift: A robust approach toward feature space analysis,' IEEE Trans. Pattern Anal. Mach. Intell., vol. 24, no. 5, pp. 603-619.
- [6] Duarte A, Sanchez A, Fernandez F, and Montemayor S (2006) Improving image segmentation quality through effective region merging using a hierarchical social metaheuristic,' Pattern Recog. Lett., vol. 27, pp. 1239-1251.
- [7] Gui C F, Li C and Xu Y (2010) 'Distance regularized level set evolution and its application to image segmentation' IEEE Trans. Image Process., vol. 19, no. 12, pp. 3243-3254. 50
- [8] Leucas Y, Wannous H and Treuillet S (2010) 'Robust tissue classification for reproducible wound assessment in telemedicine environment,' J. Electron. Imag., vol. 19, no. 2, pp. 023002-1-023002-9.
- [9] Men L, Huang M Q, and Gauch J (2013) 'Accelerating mean shift segmentation algorithm on hybrid CPU & GPU platforms,' in Proc. Int. Workshop Modern Accelerator Technol. GIScience, pp. 157-166.
- [10] Plassman P and Jones T D (2008) 'MAVIS: A non-invasive instrument to measure area and volume of wounds,' Med. Eng. Phys., vol. 20, no. 5, pp. 332-338.